Heart Rate Variability and Electrodermal Activity in Mental Stress Aloud: Predicting the Outcome

Rodrigo Lima[1,2], Daniel Osório[1,3] and Hugo Gamboa[1,2,3]

[1]*Plux-Wireless Biosignals S.A, Avenida 5 de Outubro 70, 1050-59, Lisboa, Portugal*

[2]*Department of Physics, Faculdade de Ciências e Tecnologia da Universidade Nova de Lisboa,*
Monte de Caparica, 2892-516, Caparica, Portugal

[3]*Laboratório de Instrumentação, Engenharia Biomédica e Física da Radiação (LIBPhys-UNL),*
Faculdade de Ciências e Tecnologia da Universidade Nova de Lisboa, Monte de Caparica, 2892-516, Caparica, Portugal

Keywords: Heart Rate Variability, Electrodermal Activity, Photoplethysmography, Autonomous Nervous System, Wearable Device, Biosignals, Machine-Learning, Classification.

Abstract: The assessment of changes in the autonomous nervous system (ANS), have important prognostic and diagnostic value, and can be used to assess stress levels. There are many approaches to directly measure the sympathetic and parasympathetic nervous system, although, most of them are invasive and unable to provide continuous monitoring. Heart rate variability (HRV) and Electrodermal activity (EDA) are noninvasive methods to assess the autonomous nervous system, by computing the spectral analysis of both HRV and EDA biosignals. In order to provide continuous monitoring, a wearable device is used, obtaining HRV features with photoplethysmography signals from the wrist and EDA from the fingers. The extraction of the HRV and EDA features, were obtained by submitting the subjects to a mental arithmetic stress test. The distinct response to stress was then classified using machine-learning techniques. The constructed models have the ability to predict how the subjects will respond, with an accuracy of approximately 80% in terms of HRV features in baseline and an accuracy of approximately 77% in terms of HRV and EDA simultaneous baseline features, when submitted to a situation of stress.

1 INTRODUCTION

The assessment of the changes in the autonomous nervous system (ANS) activity related with certain diseases and pathologies, such as myocardial infarction, cardiac transplantation, myocardial dysfunction, diabetic neuropathy and depression, has been demonstrated to have important prognostic and diagnostic value (Posada-Quintero et al., 2016a).

In recent times, cardiovascular research has played an important role in studying the activity of the ANS, so delineating the role of autonomous cardiac reactivity is important to prevent these serious health diseases (Posada-Quintero et al., 2016a).

The ANS is regulated by the central autonomous network in the brain, comprised of multiple neuroanatomical structures. These brain related structures influence heart activity, responding and adapting to environmental challenges, through the adjustment of physiological arousal by transmitting output to the sinoatrial node of the heart (Hamilton and Alloy, 2016).

The autonomous signals are transmitted to the body through two branches of the ANS: the sympathetic nervous system (SNS) and the parasympathetic nervous system (PNS). The sympathetic and parasympathetic nerve fibers secrete two synaptic transmitter substances: acetylcholine and epinephrine. The terminal nerve endings of the PNS secrete acetylcholine, also called cholinergic fibers, thus its influence on heart rate is mediated via release of acetylcholine by the vagus nerve, decreasing the strength of contraction and consequent heart rate (Hamilton and Alloy, 2016). The terminal endings of the SNS secrete epinephrine, also called adrenergic fibers, a term derived from adrenalin, thus its influence on the heart is mediated via release of epinephrine, increasing the force of contraction and consequent heart rate (Guyton and Hall, 2011). In a situation of stress, usually, vagal activity withdrawals, decreasing the control and influence on the heart by the vagus nerve, facilitating the activation of the SNS, with excitatory influences to the heart.

There are many approaches to directly measure the PNS and SNS activity, although, most of them are invasive and unable to provide continuous monitor-

ing, leading to an inaccurate assessment of the ANS dynamics (Posada-quintero and Hall, 2016). A non-invasive method to assess the ANS activity, is to compute the power spectral analysis of Heart Rate Variability (HRV) (Posada-Quintero et al., 2016a; Posada-Quintero et al., 2016b; Bansal et al., 2009).

HRV is a measure of the time series of beat-to-beat intervals from an electrocardiogram (ECG) between consecutive heart beats (Zoltan, 2013). HRV can also be computed by acquiring photoplethysmography (PPG) signals.

PPG is an optical measurement technique, used to detect blood volume changes in the microvascular bed of tissue, with widespread clinical application, such as ambulatory patient monitoring (Allen, 2007; Bolanos et al., 2006). PPG signals are a source of HRV information due to the synchronization between heart beats in the ECG and the systolic peak in the PPG waveform.

In order to monitor the effects of neural mechanisms to the heart, the spectral analysis of HRV has been performed to asses the level of unbalance of the ANS. The PNS is a major contributor to the high frequency (HF) component (0.15-0.4 Hz), while the low frequency (LF) component (0.04-0.15 Hz) is considered to be a marker of the sympathetic modulation, despite being influenced by both the PNS and the SNS (Zoltan, 2013; Bussmann, 1998; Miranda Dantas et al., 2012). The ratio LF/HF reflects the balance between the sympathetic and parasympathetic activity, so it has not been fully accepted as an accurate measure of the ANS, since the LF component is also influenced by the parasympathetic system (Posada-Quintero et al., 2016a).

Electrodermal Activity (EDA) is an alternative method to directly assess the SNS (Kleckner et al., 2017). The human skin is innervated by numerous efferent fibers, including sympathetic fibers, such as eccrine sweat glands, which produce sweat when the acetylcholine transmitter passes from sudomotor fibers to these glands, changing the skin's electrical characteristics (Boucsein, 2012). Eccrine glands are mostly involved in emotional responses to external stimulus and reflect only activity from the SNS, because there is no innervation of the PNS in these glands (Posada-quintero et al., 2016).

EDA signals can be divided into two different components: phasic component (SCR - Skin Conductance Response) and the tonic component (SCL - Skin Conductance Level) (Gamboa and Fred, 2008). The phasic component is the result of the activation of the SNS, after a stimuli presentation, being usually overlapped by the tonic component, which is not directly related to an external stimuli, because it is a slow changing signal (Benedek and Kaernbach, 2010).

To establish a connection between both techniques, each subject was submitted to a mental arithmetic stress test, the Paced Visual Serial Addition Test (PVSAT). The PVSAT is the visual version of the PASAT, a test where the participants are presented with a series of digits that must be summed in a narrow time interval. The participants must respond aloud the correct answer, prior to the presentation of the next digit (Tombaugh, 2006; Royan et al., 2004; Parsons and Courtney, 2014), triggering a state of anxiety and stress among the participants, increasing heart rate and electrodermal activity, making it easier to detect changes in the SNS and PNS, during the situation of stress compared to baseline.

This paper is divided in 4 sessions. In the next session the materials and methods are presented, with the description of the population, materials and protocol of the stress test performed. The methods used to analyze the data are also described in this session, with details of the algorithms used to compute HRV and EDA features. Additionally, a statistical analysis and machine-learning algorithms are also presented. Then, the results obtained are presented in session 3, with the classification and construction of the models to predict the outcome. Finally, the results obtained are discussed in session 4.

2 MATERIALS AND METHODS

2.1 Study Population

Data was acquired from a group of volunteer subjects. Fifteen participants (9 females and 6 males) of ages from 21 to 55 years old (31 ± 11), height from 1.57 to 1.85 meters (1.73 ± 0.09) and weight from 52 to 94 kilograms (72 ± 13) signed an informed consent. Table 1 gives the statistics for the study population.

Table 1: Study population statistics.

	Mean	SE	Min	Max
Age (years)	31	11	21	55
Height (m)	1.72	0.09	1.57	1.85
Weight (kg)	72	13	52	94

SE - Standard Error

2.2 Materials

The acquisition of the biosignals was made with a BITalino wearable wrist device prototype composed of six different sensors: EDA wrist, PPG, Spare sensor, Total Volatile Organic Compounds (TVOC), Car-

bon Dioxide (CO2) and Temperature (TEMP), developed by Plux Wireless Biosignals (see Table 2). For this experiment only the PPG (Channel 2) and the EDA spare sensor (Channel 3) were used. Both the PPG and EDA signals were acquired, simultaneously, with a sampling rate of 1000 Hz and 10-bit resolution. The PPG sensor is a green LED with a photodetector in reflection mode while the EDA sensor uses gelled electrodes.

(a) EDA.   (b) PPG.

Figure 1: Recording sites for the biosignals.

Table 2: Wearable Wrist Device Specifications.

Sensor	Channel	Resolution (bits)	Sampling Rate
EDA wrist	1	10	
PPG	2	10	
Spare	3	10	10 Hz
TVOC	4	10	100 Hz
CO2	5	6	1000 Hz
TEMP	6	6	

2.3 Protocol

The experiment was performed in a quiet room, in order to avoid interference that would distract the participants, due to the fact that, in order to perform the PVSAT several cognitive functions are required, such as attention and working memory. The duration of the experiment was 12 minutes (6-min baseline + 6-min stress). The stress status is defined by the changes in physiological parameters derived by the complexity and difficulty of the PVSAT, in comparison with the baseline status. The subjects were asked to sit in a comfortable chair and avoid any movement during the entire experiment, specially in the left arm. PPG and EDA signals were recorded simultaneously using the wearable device described in section 2.2. The EDA signals were recorded attaching the electrodes to the anterior middle phalanges of the 2nd finger (Position 1 in Fig.1(a)) and 3rd finger (Position 2 in Fig.1(a)) of the left hand. The PPG signal was recorded on the posterior distal left wrist, as shown in Fig.1(b).

After placing the wearable device and the EDA spare sensor, the PVSAT test was explained to the subjects. The PVSAT was presented to induce stress in the last 6-min, in a 12.2" tablet with white single numbers from 1 to 9, on a black screen. The digits were presented with a 3*s* rate for the first 2min, decreasing half a second every two minutes (2.5*s* and 2*s*). The subjects had to respond prior to the presentation of the next digit, and speak aloud each response. A warning 30s before the beginning of the PVSAT was given to all participants (Blue line in Fig.2). In baseline status, the subjects were asked not to speak.
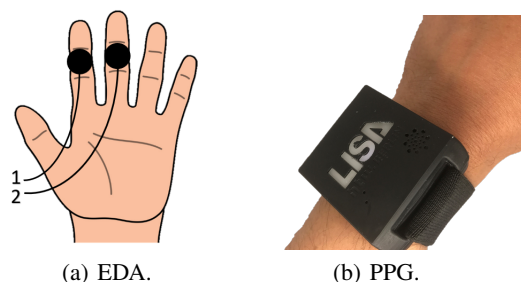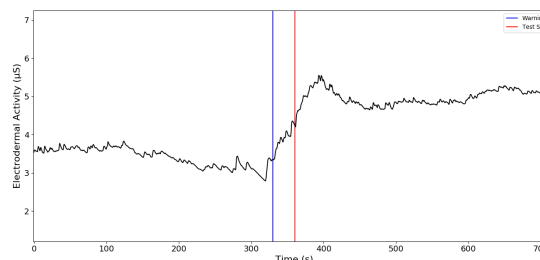
Figure 2: Representation of the warning and start of the PVSAT. EDA signal increases at the warning 30s before the PVSAT starts (Blue line). The start of the PVSAT is represented by the Red line (Brennan et al., 2001).

2.4 Data Processing

2.4.1 PPG Peak Detection

HRV features were acquired with PPG signals. In order to detect the systolic peaks in the PPG, the algorithm implemented is based on the work performed by (Kuntamalla et al., 2014). This algorithm applies a 2nd order lowpass Butterworth filter at 2 Hz, followed by a 2nd order highpass Butterworth filter at 0.1 Hz. Then it detects the peaks and valleys of the PPG wave, and computes the difference in amplitude between the peaks and the valleys. After calculating this difference, the algorithm will search for the differences that are greater than 50% of a 5-point window moving average, discarding the peaks that do not satisfy this criteria. This process is then repeated until the number of peaks between two consecutive iterations is the same. The systolic peaks detected are shown in Fig.3.

2.4.2 Heart Rate Computation

Heart rate is obtained by calculating the interval between two consecutive systolic peaks, detected with the algorithm in section 2.4.1. In order to remove artifacts influence or errors in the detection of the peaks, RR intervals lower than 380 ms were removed due to physiological conditioning, as a normal heart cycle lasts at least 380 ms. The instantaneous heart rate
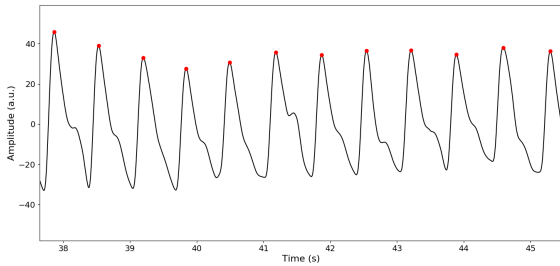
Figure 3: Peaks Detected (Red dots) with the algorithm implemented.

(IHR) in beats per minute (Bpm) is given by equation 1.

$$\text{IHR (Bpm)} = \frac{60}{\Delta RR}; \quad \Delta RR = RR_i - RR_{i-1}; \quad (1)$$

2.4.3 RR-interval Series Filtering

RR-interval series recorded from a wearable device PPG sensor are subject to different kinds of artifacts (Jang et al., 2014), as the most common are motion artifact, breathing artifact and ectopic beats, leading to a wrong detection of the R-peak (Logier et al., 2004).

To correct the miscalculated peak, a 7-point moving average window was computed. If a RR-interval differs more than 20% of the moving average, or if the RR_{i+1} is smaller than 75% of the value RR_{i-1}, those points are considered as a wrong detection (Logier et al., 2004). Then, a linear interpolation is computed to replace each interval considered as a wrong detection.

2.4.4 HRV Features

Time-domain features and frequency-domain were calculated to quantify HRV, in 5-min segments for baseline and stress. The time between the 5th and 7th minute, was considered to be the transition band, where heart rate changes significantly from baseline to stress (Fig.4).
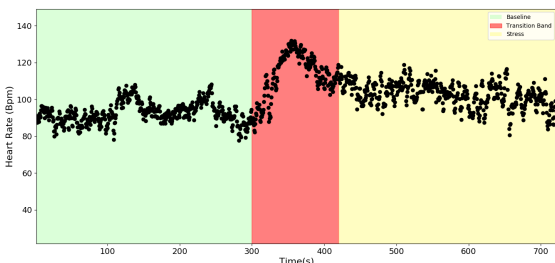
Figure 4: HRV data division in 5-min segments. Baseline status - 0-min to 5-min (Green band), Stress status - 7-min to 12-min (Yellow band). The Red band corresponds to the excluded Transition band.

Statistical features related to the variance of RR-intervals, such as SDNN, RMSSD, NN50 and pNN50, were computed for 5-min recordings (Vollmer, 2015; Guidelines, 1996).

The 5-min Poincaré plot represents the diagram in which each RR interval is plotted against the previous RR interval. From the Poincaré plot it is possible to extract non-linear variables, such as SD1, SD2 and SD2/SD1 ratio, that reflects the balance between the SNS and PNS (Hsu et al., 2012).

Frequency-domain features were also computed. The RR-interval series are an irregularly time-sampled series, though it is necessary to resample the series, to avoid the appearance of additional harmonic components in the power spectrum. Resampling was performed at a frequency of 10 Hz.

The power spectrum for baseline status (at rest) and stress status (perfoming the PVSAT) (Fig.5), was computed using a periodogram, applying to each segment, a Hanning window. Then, the Fast Fourier Transform (FFT) was calculated for each windowed segment. Very-low (VLF), low (LF), high (HF) frequency components and total power were obtained by integrating the power in each frequency band. The normalized frequency components were calculated by dividing the LF and HF power, by the total power minus the power of the VLF band (Guidelines, 1996).
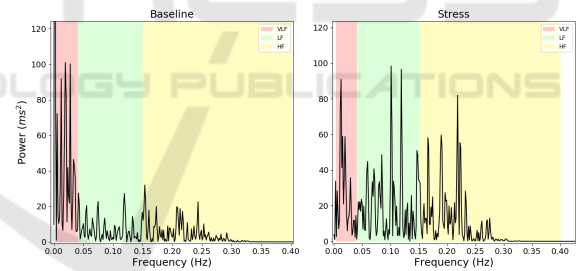
Figure 5: HRV power spectrum. The left spectrum corresponds to a Baseline status and the rigth spectrum corresponds to the Stress status. VLF (0.0033-0.04 Hz) - Red band, LF (0.04-0.15 Hz) - Green band, HF (0.15-0.4 Hz) - Yellow band.

2.4.5 EDA Features

In terms of EDA recordings, time-domain features were computed, by dividing the data into four segments: two bands of 2-min each in baseline (Baseline 1, Baseline 2) and in stress (Stress 1, Stress 2). The Red band in Fig.6, 4th to 6th minute, was considered the transition band, where EDA level changes significantly, due to the warning of the start of the PVSAT test, 30s before the start.

Time-domain features were extracted by applying a 4th order lowpass Butterworth filter at 1 Hz. Then
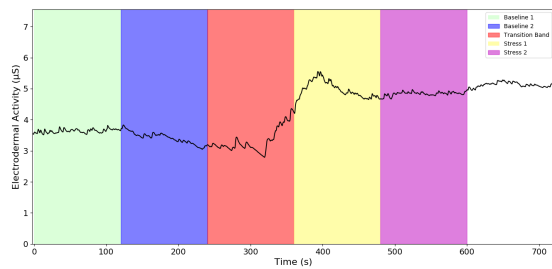
Figure 6: EDA data division in 2-min segments. Baseline 1 - 0-min to 2-min (Green Band), Baseline 2 - 2-min to 4-min (Blue band), Stress 1 - 6-min to 8min (Yellow band), Stress 2 - 8-min to 10-min (Purple band). The Red band corresponds to the Transition band.

the model proposed by (Gamboa and Fred, 2008), computed the SCR component. From the SCR waveform, time domain features such as SCR amplitude, Rise time, Recovery Time 50% (Rec.t 50%) and Recovery Time 63% (Rec.t 63%), were obtained as shown in Fig.7. A threshold of 0.005 μS was applied. The SCL component was obtained by subtracting the total EDA signal by the SCR component.
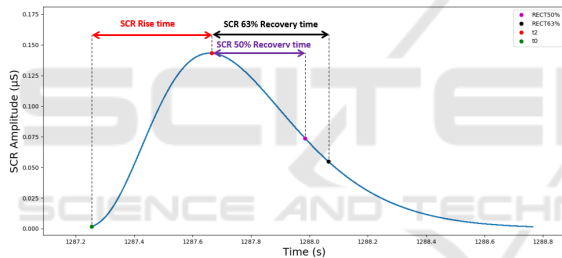
Figure 7: SCR features. The green mark corresponds to 1% of the maximum value (t0), the red mark corresponds to the maximum value of the peak (t2), the purple and the black mark correspond to the values in which the amplitude decreases, respectively, 50% and 63%.

Frequency-domain analysis was also performed (Posada-Quintero et al., 2018). After filtering the EDA signal, the signals was downsampled. Downsampling from 1000 Hz to 1 Hz was performed in three steps using consecutive factors of 1/10. Then the signals was highpass filtered with a 8th order Butterworth filter at 0.01 Hz, to remove any trend.

The power spectrum was computed using a periodogram, applying to each segment, a Blackman window. Then, the FFT was calculated for each windowed segment. The frequency band to assess the activity of the SNS through EDA used by Posada-Quintero et al., was modified to the frequency band of 0.04-0.35 Hz. Finally, the power for Band 1 (0.04-0.35 Hz) and Band 2 (0.35-0.50 Hz). The normalized frequency components were calculated by dividing Band 1 and Band 2 power, by the total power,

to verify if there was an increase in power on Band 1 during the stress situation, in order to confirm the stimulation of the SNS (Fig.8).
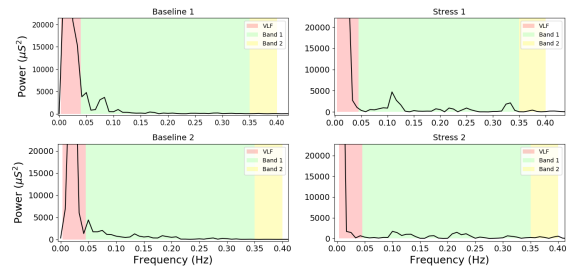
Figure 8: EDA power spectrum. VLF (0-0.045 Hz) - Red band, Band 1 (0.045-0.35 Hz) - Green band, Band 2 (0.35-0.5 Hz) - Yellow band.

2.5 Statistical Analysis

Statistical tests analysis were performed in order to assess the significance of the results obtained, between the baseline and stress features.

Kruskal-Wallis test is a non-parametric test, so it means that is does not assume the normality of data nor the homoscedaticity (standard deviation are equal). The H-test uses ranked values, so the values observed are converted to their ranks. The Kruskal-Wallis null-hypothesis is that the mean ranks of the different groups are the same (McDonald, 2014). Probabilities lower than the significance level of 5% (*p-value*< 0.05) were considered significant, concluding that the null hypothesis may not adequately explain the observation - there is in fact variation between the ranked means of the groups.

Chi-square test χ^2 was also applied to test the goodness of fit in section 3.2. This test is applied to determine whether a categorical variable from a single population is consistent with a hypothesized distribution. The null hypothesis is that the categorical data has the given frequencies (Cochran, 2013). In the context of this paper, the χ^2 test will be applied to determine the goodness of the fit of the linear regression line performed, by comparing the values observed calculated using the regression line obtained, with the expected values. Probabilities higher than the significance level of 5% (*p-value*< 0.05) lets us conclude that the difference between the observed values and the expected values is minimized, so the linear regression is a good fit.

2.6 Machine-Learning

Machine-learning algorithms were applied in order to classify the data.

Support Vector Machines (SVM) algorithms for learning two-class discriminant functions from a set of training examples were applied, in order to find a suitable boundary (hyperplane), in data space to separate two classes. The basis of this boundary is the concept of margin, which is the minimal distance between the hyperplane separating the two classes and the closest points to it, defined as the support vectors. In linearly separable data, the kernel of SVM used is the maximal margin classifier or hard margin SVM (Vapnik, 1999).

Random Forest classifiers are based on the Decision Tree algorithm. Decision Trees are a supervised method of classification in machine learning, using pre-classified data. The division of the data is based on the values of features of the given data, by deciding which features, best divide ir, creating a set of rules for the values of each feature. The Random Forest classifier is a combination of multiple decision trees, where each decision tree is made by randomly selecting portions of the data, reducing the correlation between trees, improving the prediction power and results with a higher efficiency (Breiman, 2001; Donges, 2018).

3 RESULTS

The results obtained showed that the PVSAT induced stress to the subjects, reflected by the increase in heart rate and in EDA features, such as SCR and SCL, during stress.

Frequency analysis of EDA, also confirmed the activation of the sympathetic nervous system with an increase in Band 1 power in stress.

For HRV, the results obtained for spectral measures were opposite to the expected. It was expected to verify an increase in LF(nu) and LF/HF ratio during stress, but no significant result was found for frequency-domain features.

Despite no significance was obtained in frequency-domain features for HRV, a thorough analysis of these spectral characteristics, revealed that in some subjects the LF(nu) decreased in stress, while in other subjects there was an increase in stress. Actually, within the 15 subjects that were analyzed, there was a division of 8 subjects in which LF(nu) decreased during stress, and 7 subjects that LF(nu) increased during stress. So, when analyzing the group as a whole, it is possible that the opposite responses cancels out the LF(nu) results. Therefore, two distinct groups were formed: group 1 consisted of subjects which LF(nu) decreased during stress, and group 2 consisted of subjects which LF(nu)

increased during stress. Then, all features for HRV were analyzed for each group.

For group 1, the results showed a significant increase in HF(nu) power, LF(nu) power and LF/HF ratio. For group 2, the results showed significant effect only for Bpm and RR interval .

3.1 Support Vector Machines

In this section, SVM were applied to try separate by a hyperplane the two different responses of the subjects to stress: decrease in LF(nu) and increase in LF(nu) (see Fig.9). This separation is based on the work of Vuksanovic et al. (Vuksanović and Gal, 2007), that verified this distinct response to stress, but in respect to HF power.

First, a binary classification of each group was applied: Group 1 - Decrease in LF(nu) was classified as $Y = -1$ and Group 2 - Increase in LF(nu) was classified as $Y = 1$. The decision function obtained to separate the two groups is given by equation 2, where w_1 and w_2 represents, respectively, the weights for groups 1 and 2, $\vec{x_1}$ and $\vec{x_2}$ represents, respectively, a point for group 1 (Blue circles in Fig.9) and group 2 (Red circles in Fig.9).

$$w_1.\vec{x_1} + w_2.\vec{x_2} + b = 0 \qquad (2)$$

The results obtained for the weights and the b parameter were: $w_1 = -0.31$, $w_2 = 0.25$ and $b = 4.85$. The number of support vectors for each group were: Group 1 - 1 support vector, Group 2 - 2 support vectors. The coordinates ([LF(nu) Baseline, LF(nu) Stress]) of the support vectors (Black not filled circles in Fig.9) for each group were: Group 1 - [78.48,74.64] and in Group 2 - [77.35,81.25];[63.08,63.41].
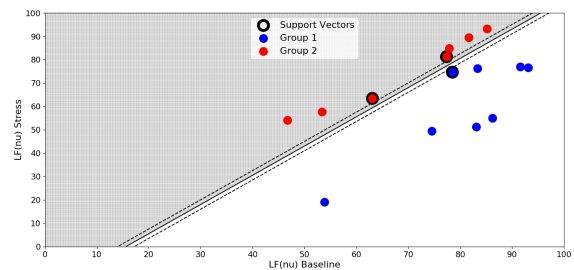
Figure 9: SVM Group Separation by the hyperplane: $-0.31.\vec{x_1} + 0.25.\vec{x_2} + 4.85 = 0$. Blue circles - Group 1. Red circles - Group 2. The support vectors are the points with black border.

3.2 Linear Regression

In session 3.1, the results showed that the responses of the groups were parallel, so it was possible to predict the LF (nu) values during stress based on the baseline values for each group separately. A linear regression was then computed for each group (Fig.10). For Group 1 regression (Red line in Fig.10), the following regression line was obtained: LF(nu) Stress $= 1.40 \times$ LF(nu) Baseline $- 53.15, r^2 = 0.728$. For Group 2 regression (Blue line in Fig.10), the regression line obtained was LF(nu) Stress $= 1.06 \times$ LF(nu) Baseline $+ 1.48, r^2 = 0.972$.

Finally, a chi-squared test for goodness of fit was applied to the regression lines, comparing the expected values with the observed values using the regression line obtained. For group 1 the chi-square result was $\chi^2(6) = 12.785; p = 0.047$ and for group 2 was $\chi^2(5) = 0.674; p = 0.984$. With the results obtained for the χ^2 statistic, it is possible to reject at a significance level of 5%, the null hypothesis for group 1, concluding that the fit of the regression line is not adequate, while for group 2, with a *p-value*=0.984 it is possible to accept the null hypothesis, concluding that the fit of the regression line is suitable.
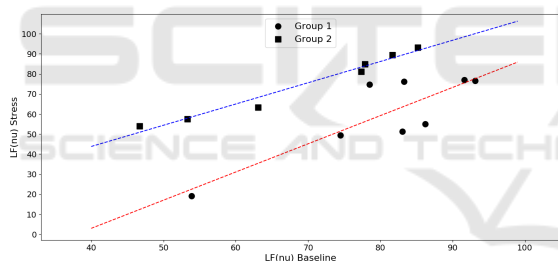
Figure 10: Linear Regression for each group. Group 1 regression line (Red line): LF(nu) Stress $= 1.40 \times$ LF(nu) Baseline $- 53.15, r^2 = 0.728$; Group 2 regression line (Blue line): LF(nu) Stress $= 1.06 \times$ LF(nu) Baseline $+ 1.48, r^2 = 0.972$.

3.3 Random Forest Classifier

In section 3.1, it was possible to separate the subjects into two groups, by evaluating their response to stress, with an increase or a decrease in LF(nu) during stress. As this separation is based on a frequency-domain feature, requiring the recording of the data for at least 10 minutes (5-min in baseline, 5-min in stress), in order to predict the subject's response to a situation of stress in a shorter recording time, a classification of the subjects using only time-domain features for both HRV and EDA, was performed, to classify the subjects into the two different groups obtained in the previous section.

This classification was performed with a random forest classifier, with 10 decision trees, and a Gini criteria to assess the impurity and the quality of the split. Training of the classifier was performed with a cross validation method, using 6 different random splits and a test sample of 30% of the subjects. This process was repeated 100 times, so that it was possible to choose the model that best classifies the data, that is, the model with a higher accuracy score for the cross validation training method.

First, a random forest classifier using only the following time-domain features for HRV was performed: Bpm, RR-interval and SD2/SD1 ratio. Then, the importance of each feature is plotted in figure 11. From this figure, we verify that RR-interval is the most important feature in this model, followed by the SD2/SD1 ratio and the Bpm. The accuracy score for this model to classify correctly each subject to the corresponding group was approximately 80%.
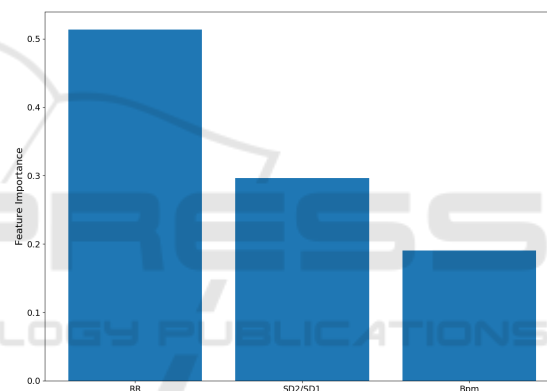
Figure 11: Feature Importance for HRV features obtained with the random forest classifier.

In order to obtain a better visualization of the regions defined by the random forest classifier, the features boundaries are shown in a 3D graph (Fig. 12). A subject with features coordinates that belong to the blue region will be assigned to group 1 - decrease in LF(nu), and subjects that belong to the red region will be assigned to group 2 - Increase in LF(nu).
Information related to EDA was added to the classifier. Similarly to the previous classifier, in order to reduce the recording time, only time-domain features for EDA were added to the classifier. The following features for EDA were selected: SCR, SCL and Rise Time. The more accurate estimators were selected, with the corresponding decision trees. The importance of each feature in plotted in figure 13. The accuracy score for this model was approximately 77%.
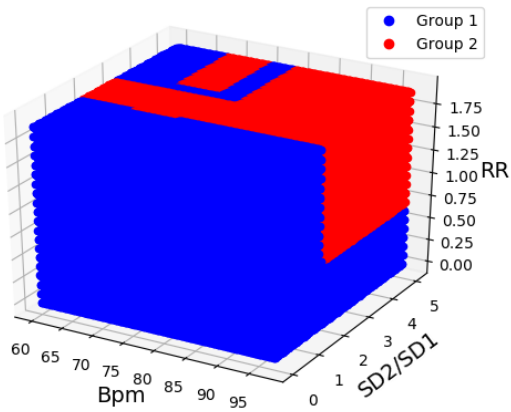
Figure 12: 3D Decision Surface for the Random Forest Classifier. Features selected: Bpm, SD2/SD1 and RR-interval (s). Blue region - Group 1 and Red region - Group 2.
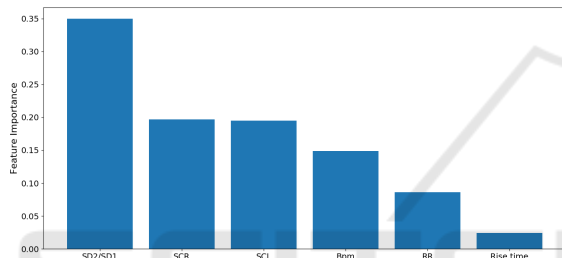
Figure 13: Feature Importance for HRV and EDA features obtained with the random forest classifier.

4 DISCUSSION

This was a pilot study to see the influence of stress induction on the autonomous nervous system, by processing HRV and EDA from a wearable device.

The results obtained in section 3, showed that the arithmetic test (PVSAT) induced stress to the subjects, reflected by the increase in heart rate (Bpm) and in EDA features, such as, SCR and SCL, during stress.

For EDA features, SCR, SCL, Rise time, Rec.t 50% and Rec.t 63%, revealed to be good markers of stress, with the increase of values during all the segments studied during stress compared to the baseline segments. In section 2.4.5, the frequency analysis of EDA signals was performed to confirm the activation of the sympathetic nervous system with an increase in power for low frequency bands. The results obtained showed that there was a significant increase in Band 1 power. This confirms that the dynamics of the sympathetic nervous system are confined to low frequencies, in agreement with the work performed by Posada et al., although in this paper the frequency

band studied was extended more 0.10 Hz, the increase in power was also verified, making frequency analysis of EDA a potential marker of quantitative assessment of the level of stress and sympathetic nervous system impairments (Posada-Quintero et al., 2016a).

For HRV, the results obtained for spectral measures were opposite to the expected. The inducement of stress in subjects was expected to increase LF(nu) and LF/HF ratio (Visnovcova et al., 2013; Hjortskov et al., 2004; Vuksanović and Gal, 2007). Contrarily to the expectation, the results obtained showed that there was a decrease in LF(nu) and LF/HF ratio during stress, results also reported by (Tharion et al., 2009; Vuksanović and Gal, 2007; Hjortskov et al., 2004). Vuksanovic et al. reported that vocalization of the answers, assigned to parasympathetic activity, during the PVSAT interfered with the spectral analysis and concealed out the changes in spectral measures of HRV (Vuksanović and Gal, 2007). Langewitz et al. showed that the breathing pattern for some subjects during vocalization affects the low frequency band power, as the breathing frequency falls in the 0.1 Hz frequency band, the resonance phenomenon will not increase the power in the LF band (Langewitz and Ruddel, 1989), concluding that the fact subjects answered the PVSAT aloud might have influenced the spectral measures of HRV. These facts also show that the LF band does not reflect purely the cardiac response to the activation of the sympathetic nervous system, but a mixture of the sympathetic and parasympathetic systems, with counteracting effects of activation of the sympathetic system and withdrawal of the parasympathetic system (Sloan et al., 1991). From the point of view of humoral mechanisms, these results can be explained, as, during a situation of stress, the sympathetic nervous system affects the heart through release of catecholamines (Terkelsen et al., 2005), such as epinephrine, leading to an increase in heart rate without changing heart rate variability measures, as the release of epinephrine does not affect spectral measures (Ahmed et al., 1994).

In section 3.1, despite the results for HRV were concealed out when analyzing the subjects as a whole, it was possible to verify significant changes in spectral measures for HRV after separating the subjects into the two different groups, based on the work performed by Vuksanovic et al., and as an exploratory method in order to find a pattern, taking into account that subjects can exhibit distinct response when submitted to stress. From figure 10, it is possible to see that the slopes for each group do not intercept with one another, so the two responses are parallel. For group 2, the results obtained were in agreement with

the expectations that during stress, the LF(nu) and the LF/HF ratio increased with a small decrease in HF(nu) power with no significance. This group responds to stress with the withdrawal of the parasympathetic nervous system and the activation of the sympathetic nervous system. For group 1, the results showed significant decrease in LF(nu) and LF/HF ratio during stress and significant increase in HF(nu) power. The simultaneous increase in HF(nu) and heart rate is more difficult to explain, although it could be an influence of complex respiratory pattern (Vuksanović and Gal, 2007), or it could be the effect of different co-activation humoral mechanims, caused by compensatory sympatho-adrenal activation with catecholamine release into the circulation (Terkelsen et al., 2005).

In terms of EDA, both groups showed an increase in Band 1 power, although significance was only found in group 2 between baseline 2 and stress 1 segments. It is possible to conclude that even if there is a distinct response to stress in terms of HRV, there is activation of the sympathetic nervous system during the stress situation, due to the fact that the sympathetic nervous system influences the heart and sweat through distinct hormones, respectively, epinephrine and acetylcholine.

Finally, the classification model implemented in section 3.3, showed that it was possible to predict the type of response for each subject during stress, using only their baseline features for both HRV and EDA features, making it possible to classify the subjects into the two different groups, with an accuracy of approximately 80% for HRV features in baseline and an accuracy of approximately 77% for HRV and EDA simultaneous features. This model assumes to be a good asset for future assessment of the type of response when the subjects are under a stress situation.

REFERENCES

Ahmed, M. W., Kadish, A. H., Parker, M. A., and Goldberger, J. J. (1994). Effect of physiologic and pharmacologic adrenergic stimulation on heart rate variability. *Journal of the American College of Cardiology*, 24(4):1082–1090.

Allen, J. (2007). Photoplethysmography and its application in clinical physiological measurement. *Physiological Measurement*, 28(3).

Bansal, D., Khan, M., and Salhan, A. (2009). A Review of Measurement and Analysis of Heart Rate Variability. In *2009 International Conference on Computer and Automation Engineering*, pages 243–246.

Benedek, M. and Kaernbach, C. (2010). A continuous measure of phasic electrodermal activity. *Journal of Neuroscience Methods*, 190(1):80–91.

Bolanos, M., Nazeran, H., and Haltiwanger, E. (2006). Comparison of heart rate variability signal features derived from electrocardiography and photoplethysmography in healthy individuals. In *Annual International Conference of the IEEE Engineering in Medicine and Biology - Proceedings*, pages 4289–4294.

Boucsein, W. (2012). *Electodermal Activity*. Second edi edition.

Breiman, L. (2001). Random forests. *Machine Learning*, 45(1):5–32.

Brennan, M., Palaniswami, M., and Kamen, P. (2001). Do existing measures of Poincareé plot geometry reflect nonlinear features of heart rate variability? *IEEE Transactions on Biomedical Engineering*, 48(11):1342–1347.

Bussmann, B. (1998). Differentiation of autonomic nervous activity in different stages of coma displayed by power spectrum analysis of heart rate variability. pages 46–52.

Cochran, W. G. (2013). The χ2 Test of Goodness of Fit. *The Annals of Mathematical Statistics*, 23(3):315–345.

Donges, N. (2018). The Random Forest Algorithm.

Gamboa, H. and Fred, A. (2008). Electrodermal Activity Model. *Psychophysiology*, (April):30.

Guidelines (1996). Guidelines Heart rate variability. *European Heart Journal*, 17:354–381.

Guyton, A. C. and Hall, J. E. (2011). *Textbook of Medical Physiology*.

Hamilton, J. L. and Alloy, L. B. (2016). Atypical reactivity of heart rate variability to stress and depression across development: Systematic review of the literature and directions for future research.

Hjortskov, N., Rissén, D., Blangsted, A. K., Fallentin, N., Lundberg, U., and Søgaard, K. (2004). The effect of mental stress on heart rate variability and blood pressure during computer work. *European Journal of Applied Physiology*, 92(1-2):84–89.

Hsu, C. H., Tsai, M. Y., Huang, G. S., Lin, T. C., Chen, K. P., Ho, S. T., Shyu, L. Y., and Li, C. Y. (2012). Poincaré plot indexes of heart rate variability detect dynamic autonomic modulation during general anesthesia induction. *Acta Anaesthesiologica Taiwanica*, 50(1):12–18.

Jang, D.-G., Park, S., Hahn, M., and Park, S.-H. (2014). A Real-Time Pulse Peak Detection Algorithm for the Photoplethysmogram. *International Journal of Electronics and Electrical Engineering*, 2(1):45–49.

Kleckner, I. R., Jones, R. M., Wilder-Smith, O., Wormwood, J. B., Akcakaya, M., Quigley, K. S., Lord, C., and Goodwin, M. S. (2017). Simple, Transparent, and Flexible Automated Quality Assessment Procedures for Ambulatory Electrodermal Activity Data.

Kuntamalla, S., Ram, L., and Reddy, G. (2014). An Efficient and Automatic Systolic Peak Detection Algorithm for Photoplethysmographic Signals. *International Journal of Computer Applications*, 97(19):975–8887.

Langewitz, W. and Ruddel, H. (1989). Spectral analysis of heart rate variability under mental stress. *J Hypertens Suppl*, 7(6):S32—-3.

Logier, R., De Jonckheere, J., and Dassonneville, A. (2004). An efficient algorithm for R-R intervals series filtering. *Conference proceedings : ... Annual International Conference of the IEEE Engineering in Medicine and Biology Society. IEEE Engineering in Medicine and Biology Society. Conference*, 6:3937–3940.

McDonald, J. H. (2014). Kruskal–Wallis test - Handbook of Biological Statistics.

Miranda Dantas, E., Lima Sant'Anna, M., Varejão Andreão, R., Pereira Gonçalves, C., Aguiar Morra, E., Perim Baldo, M., Lamêgo Rodrigues, S., and Geraldo Mill, J. (2012). Spectral analysis of heart rate variability with the autoregressive method: What model order to choose? *Computers in Biology and Medicine*, 42(2):164–170.

Parsons, T. D. and Courtney, C. G. (2014). An initial validation of the Virtual Reality Paced Auditory Serial Addition Test in a college sample. *Journal of Neuroscience Methods*, 222:15–23.

Posada-Quintero, H., Florian, J., Orjuela-Cañón, A., and Chon, K. (2018). Electrodermal activity is sensitive to cognitive stress under water. *Frontiers in Physiology*, 8(JAN):1–8.

Posada-Quintero, H. F., Florian, J. P., Orjuela-Cañón, A. D., Aljama-Corrales, T., Charleston-Villalobos, S., and Chon, K. H. (2016a). Power Spectral Density Analysis of Electrodermal Activity for Sympathetic Function Assessment. *Annals of Biomedical Engineering*, 44(10):3124–3135.

Posada-Quintero, H. F., Florian, J. P., Orjuela-Cañón, Á. D., and Chon, K. H. (2016b). Highly sensitive index of sympathetic activity based on time-frequency spectral analysis of electrodermal activity. *American Journal of Physiology - Regulatory, Integrative and Comparative Physiology*, 311(3):R582–R591.

Posada-quintero, H. F. and Hall, S. (2016). Electrodermal Activity : What it can contribute to the Assessment of the Autonomic Nervous System. page 24.

Posada-quintero, H. F., Member, S., Chon, K. H., and Member, S. (2016). Frequency - Domain Electrodermal Activity Index of Sympathetic Function. pages 497–500.

Royan, J., Tombaugh, T. N., Rees, L., and Francis, M. (2004). The Adjusting-Paced Serial Addition Test (Adjusting-PSAT): Thresholds for speed of information processing as a function of stimulus modality and problem complexity. *Archives of Clinical Neuropsychology*, 19(1):131–143.

Sloan, R. P., Korten, J. B., and Myers, M. M. (1991). Components of heart rate reactivity during mental arithmetic with and without speaking. *Physiology and Behavior*, 50(5):1039–1045.

Terkelsen, A. J., Mølgaard, H., Hansen, J., Andersen, O. K., and Jensen, T. S. (2005). Acute pain increases heart rate: Differential mechanisms during rest and mental stress. *Autonomic Neuroscience: Basic and Clinical*, 121(1-2):101–109.

Tharion, E., Parthasarathy, S., and Neelakantan, N. (2009). Short-term heart rate variability measures in students during examinations. *National Medical Journal of India*, 22(2):63–66.

Tombaugh, T. N. (2006). A comprehensive review of the Paced Auditory Serial Addition Test (PASAT). *Archives of Clinical Neuropsychology*, 21(1):53–76.

Vapnik, V. N. (1999). An overview of statistical learning theory. *IEEE transactions on neural networks / a publication of the IEEE Neural Networks Council*, 10(5):988–99.

Visnovcova, Z., Calkovska, A., and Tonhajzerova, I. (2013). Heart Rate Variability and Electrodermal Activity As Noninvasive Indices of Sympathovagal Balance in Response To Stress. *Acta Medica Martiniana*, 13(1):5–13.

Vollmer, M. (2015). A robust, simple and reliable measure of heart rate variability using relative RR intervals. *Computing in Cardiology*, 42(6):609–612.

Vuksanović, V. and Gal, V. (2007). Heart rate variability in mental stress aloud. *Medical Engineering and Physics*, 29(3):344–349.

Zoltan, G.-S. (2013). Wavelet transform based HRV analysis. *The 7th International Conference Interdisciplinarity in Engineering (INTER-ENG 2013)*, 12:105–111.